genes. The L110P and E148Q mutations on MEFV were considered to be single-nucleotide polymorphisms (SNPs), based upon the prevalence of the mutations, as well as their weak association with FMF in Japan. Because none of periodic fever, rashes, gastrointestinal symptoms, or elevated serum IgD was observed at that time, the MVK gene was not examined.

The patient continued to show a good response to the AIH treatments, although tapering off the prednisone induced periodic fever with maculopapular rashes approximately once a month, shown for the first time at the age of 32 months. The fever episodes persisted for 3–5 days and the duration of the fever was reduced to 1–2 days by temporarily increasing the dose of prednisone. Serum CRP levels were around 20 mg/dl at the onset of fever, and 1–4 mg/dl in the asymptomatic period. The newly emerged clinical symptoms and the good response to the systemic steroid prompted us to consider HIDS. Full examination for HIDS showed: (1) elevated serum IgD (19.2 mg/dl) (control 0–9 mg/dl); (2) increased urinary mevalonic acid (49.1 μg/mg creatinine) (control 0.091 ± 0.028 μg/mg creatinine); and (3) a significant decrease in the mevalonate kinase activity of peripheral blood mononuclear cells (PBMCs; below the detection limit). Genetic analysis of the MVK gene revealed compound heterozygous mutations, A262P and H380R, the former of which was a novel mutation (Fig. 2b). The MVK mutations were not identified in 100 healthy Japanese controls. Finally we diagnosed the patient with HIDS, at the age of 6 years. We treated the patient with simvastatin (0.07 mg/kg/day), which was partially effective in reducing the frequency of the periodic fever. Although no decline in urinary mevalonic acid has been produced by simvastatin (33.7–107.8 μg/mg creatinine), the patient has had a benign course, without mental retardation or neurological impairments (Fig. 3).

To see if the patient's liver abnormalities were due to either AIH or HIDS, we performed an immunohistological analysis of the biopsied liver specimen. It was stained for CD68, and unstained for CD3 and CD79 (Fig. 4). These

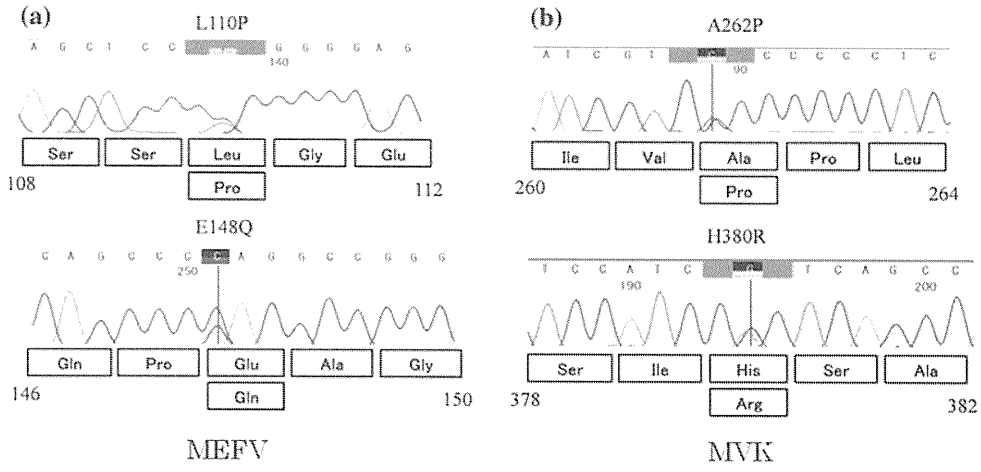

Fig. 2 Genetic analysis. **a** Genetic analysis of the MEFV gene. The patient had heterozygous amino acid changes of L110P and E148Q. **b** Genetic analysis of the MVK gene. The patient had heterozygous mutations of A262P and H380R

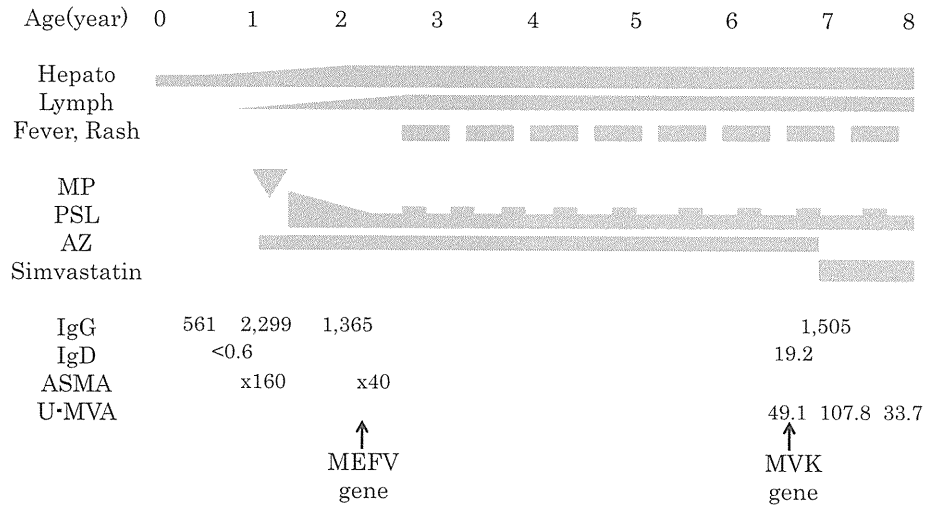

Fig. 3 Clinical course. *Hepato* Hepatosplenomegaly, *Lymph* cervical lymphadenopathy, *MP* methylprednisolone, *PSL* prednisolone, *AZ* azathioprine, *ASMA* anti-smooth muscle antibody, *U-MVA* urinary mevalonic acid (μg/mg creatinine)

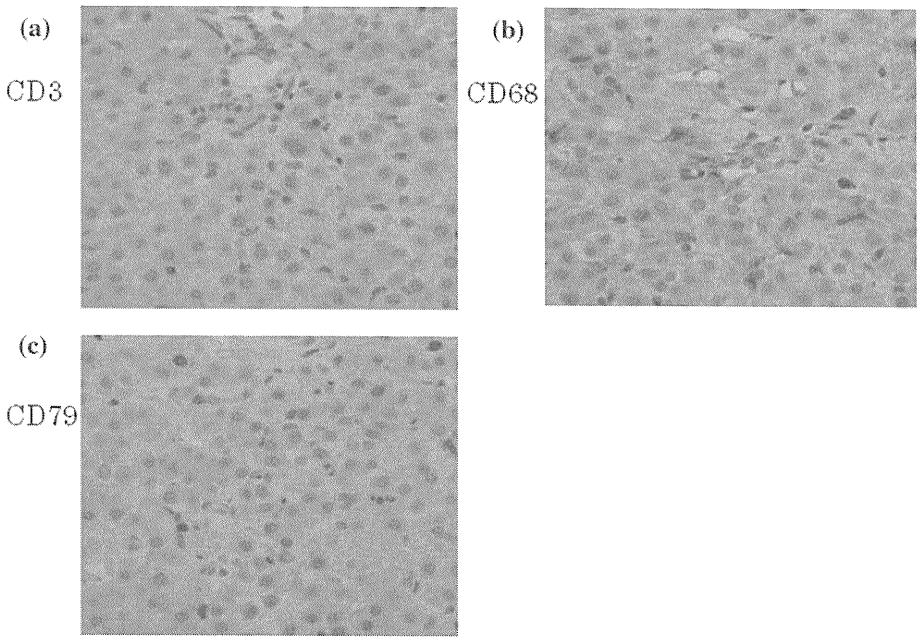

Fig. 4 Immunohistochemical analysis of the biopsied liver tissues. **a** CD3 (×400), **b** CD68 (×400), **c** CD79 (×400)

data led us to conclude that the hepatitis seemed to be a manifestation of HIDS, rather than resulting from an autoimmune response.

Discussion

We have reported here a Japanese girl who was diagnosed with HIDS by genetic analysis, as well as by laboratory examinations such as mevalonate kinase activity and urinary excretion of mevalonate. According to the report of the Japanese HIDS registry, the 4 most prevalent MVK mutations (V377I, I268T, H20P/N, and P167L) accounted for 71.5% of the mutations found. Our patient had a very rare genotype among the patients on the HIDS registry, as the H380R mutation was identified in 1.5% of the patients and A262P was a novel mutation. Because mevalonate kinase activity was below the detection limit, mevalonic aciduria could have been considered as the diagnosis in our patient. However, the mevalonic acid level in the urine was not as high as that reported for patients with mevalonic aciduria [4] and the clinical features of our patient lacked the neurological and developmental abnormalities that are distinctive signs of mevalonic aciduria. Thus, we concluded that the patient suffered from a severe form of HIDS, although we note that mevalonate kinase deficiency presents as a phenotypic continuum in which disease severity ranges from mevalonic aciduria to HIDS [5].

Serum transaminase levels in our patient were elevated since birth, which is relatively rare for HIDS, and liver biopsy showed chronic non-specific hepatitis [6]. Although the serum transaminase levels were improved by the treatment for AIH, the histological and immunohistochemical findings were not typical of AIH [6], which is a generally unresolving inflammation of the liver of unknown cause [7]. There have been some reports of HIDS patients with liver abnormalities. Topaloglu et al. [8] reported a similar case of HIDS in a patient who had neonatal hepatosplenomegaly without fever at the beginning, and they performed liver biopsy which showed portal fibrosis. Hinson et al. [9] reported two patients with mevalonate kinase deficiency who had neonatal hepatosplenomegaly and elevated transaminase levels; liver biopsy showed chronic active cholestatic hepatitis and portal fibrosis, respectively.

Neonatal hepatitis is a syndrome associated with a history that includes any type of infectious, genetic, toxic, or metabolic causation. Neonatal hepatitis is characterized by clinical and laboratory findings of liver dysfunction, particularly conjugated hyperbilirubinemia. In our patient, the clinical course in early childhood was not typical of neonatal hepatitis. But the clinical course in our patient suggests that it is important to include HIDS in the differential diagnosis of neonatal hepatitis or neonatal-onset chronic hepatitis.

Genetic analysis of autoinflammatory disease genes in our patient revealed 2 heterozygous amino acid changes, L110P and E148Q, in the MEFV gene, which were shared with the patient's asymptomatic mother. It has been reported that the allele frequency of E148Q in the Japanese population was high (16.38%), and both E148Q and L110P are considered as SNPs [10]. On the other hand, Touitou et al. [11] demonstrated that E148Q may have an exacerbating effect on FMF when it is part of complex alleles. In addition, there are other reports that mutations in 2 autoinflammatory

genes cause more severe diseases [8, 12]. Thus, the heterozygous E148Q and L110P amino acid changes in the MEFV gene may cause a more severe form of HIDS.

The name 'HIDS' was given to the disorder because of the observed elevation in serum IgD, before the identification of the disease-causing mutations in the MVK gene. In a study of 103 HIDS patients, 22% had normal serum IgD, particularly during infancy [13], which indicates that serum IgD is not sensitive enough for diagnosing HIDS. In Asian countries like Japan, HIDS is so rare that clinicians do not know the clinical relevance of IgD in relation to the diagnosis of HIDS. Therefore, it is very important to let clinicians know that more specific and more sensitive diagnostic tests; namely, measurement of urinary mevalonic acid and/or genetic analysis of the MVK gene are necessary to diagnose HIDS. It should also be pointed out that both the measurements of urinary mevalonic acid and the genetic tests of the MVK gene require special laboratory equipment, which makes it difficult to access such diagnostic tests.

In conclusion, we have reported a patient with a severe form of HIDS who presented with neonatal-onset chronic hepatitis with a novel MVK mutation. HIDS should be included in the differential diagnosis of neonatal-onset chronic hepatitis, even if the serum IgD is within the normal range and typical recurrent fever is not identified.

Acknowledgments We are grateful to Dr. Hans R. Waterham for measurement of mevalonate kinase activity.

Conflict of interest The authors have no conflicts of interest to declare.

References

1. Drenth JP, Denecker NE, Prieur AM, van der Meer JW. Hyperimmunoglobulin D syndrome. Presse Med. 1995;24:1211–3.
2. Alvarez F, Berg PA, Bianchi FB, Bianchi L, Burroughs AK, Cancado EL, et al. International Autoimmune Hepatitis Group report: review of criteria for diagnosis of autoimmune hepatitis. J Hepatol. 1999;31:929–38.
3. Sogo T, Fujisawa T, Inui A, Komatsu H, Etani Y, Tajiri H, et al. Intravenous methylprednisolone pulse therapy for children with autoimmune hepatitis. Hepatol Res. 2006;34:187–92.
4. Houten SM, Wanders RJA, Waterham HR. Biochemical and genetic aspects of mevalonate kinase and its deficiency. Biochim Biophys Acta. 2000;1529:19–32.
5. Simon A, Kremer HPH, Wevers RA, Scheffer H, de Jong JG, van der Meer JWM, et al. Mevalonate kinase deficiency: evidence for a phenotypic continuum. Neurology. 2004;62:994–7.
6. Kage M. Pathology of autoimmune liver diseases in children. Hepatol Res. 2007;37:S502–8.
7. Manns MP, Czaja AJ, Gorham JD, Krawitt EI, Mieli-Vergani G, Vergani D, et al. Diagnosis and management of autoimmune hepatitis. Hepatology. 2010;51:2193–213.
8. Topaloglu R, Ayaz NA, Waterham HR, Yuce A, Gumruk F, Sanal O. Hyperimmunoglobulinemia D and periodic fever syndrome; treatment with etanercept and follow-up. Clin Rheumatol. 2008;27:1317–20.
9. Hinson DD, Rogers ZR, Hoffmann GF, Schachtele M, Fingerhut R, Kohlschtter A, et al. Hematological abnormalities and cholestatic liver disease in two patients with mevalonate kinase deficiency. Am J Med Genet. 1998;78:408–12.
10. Komatsu M, Takahashi T, Uemura N, Takada G. Familial Mediterranean fever medicated with an herbal medicine in Japan. Pediatr Int. 2004;46:81–4.
11. Touitou I. The spectrum of familial Mediterranean fever (FMF) mutations. Eur J Hum Genet. 2001;9:473–83.
12. Stojanov S, Lohse P, Lohse P, Hoffmann F, Renner ED, Zellerer S, et al. Molecular analysis of the MVK and TNFRSF1A genes in patients with a clinical presentation typical of the hyperimmunoglobulinemia D with periodic fever syndrome: a low-penetrance TNFRSF1A variant in a heterozygous MVK carrier possibly influences the phenotype of hyperimmunoglobulinemia D with periodic fever syndrome or vice versa. Arthritis Rheum. 2004;50:1951–8.
13. Van der Hilst JC, Bodar EJ, Barron KS, Frenkel J, Drenth JP, van der Meer JW, International HIDS Study Group, et al. Long-term follow-up, clinical features, and quality of life in a series of 103 patients with hyperimmunoglobulinemia D syndrome. Medicine (Baltimore). 2008;87:301–10.

Review Article

Autoinflammatory diseases - a new entity of inflammation

Toshio Heike[1,*], Megumu K Saito[2], Ryuta Nishikomori[1], Takahiro Yasumi[1] and Tatsutoshi Nakahata[2]

[1]Department of Pediatrics, Graduate School of Medicine, Kyoto University, Kyoto, Japan
[2]Clinical Application Department, Center for iPS cell research and application, Kyoto University, Kyoto, Japan

The autoinflammatory diseases are characterized by seemingly unprovoked episodes of inflammation, without high-titer autoantibodies or antigen-specific T cells. The concept was proposed ten years ago with the identification of the genes underlying hereditary periodic fever syndromes. NLRP3 inflammasome activation and IL-1β secretion have recently emerged as a central mechanism in the pathogenesis of disease. Here we describe four genetically defined syndromes like cryopyrin-associated periodic syndromes (CAPS, cryopyrinopathies), mevalonate kinase deficiency (MKD) or hyper-IgD and periodic fever syndrome (HIDS), pyogenic aseptic arthritis, pyoderma gangrenosum, and acne syndrome (PAPA syndrome), and deficiency of interleukin-1-receptor antagonist (DIRA) along with the pitfall for understanding the pathphysiology.

Rec./Acc.2/7/2011

*Correspondence should be addressed to:
Toshio Heike

Key words:
autoinflammatory disease, NLRP3 inflammasome, IL-1β, cryopyrin-associated periodic fever (CAPS), mosaicism

Introduction

Inflammation has evolved as a physiologic mechanism necessary to defend our bodies from external and internal danger triggers such as infectious agents, chemical factors, and physical factors [1].

The innate immune system is assigned to recognize and encounter these stimuli. Recently, nucleotide-binding oligomerization domain (NOD)-like receptors (NLRs) have emerged as key players for the proper accomplishment of this process through recognition of pathogen associated molecular patterns (PAMPs) [2]. In addition to PAMPs, NLRs also sense endogenous stress signals known as damage associated molecular patterns (DAMPs) [2,3]. NLR dependent recognition of either exogenous or endogenous danger signals

initiates the recruitment of adaptor proteins and the formation of molecular platforms referred to as inflammasomes[2, 3]. In other word, inflammasomes are cellular alarts that assemble in response to microbial invasion and/or cellular damage and alert the system by triggering an inflammatory response. The subsequent activation of caspase-1 results in the post-transcriptional, proteolytic modulation of the related cytokines interleukin-1β (IL-1β) and IL-18 from their precursor to their active and secreted form, enhancing the inflammatory process. Among severalNLRs that form inflammasome platforms, the most studied are NALP1,NALP3 (NLRP3) and IPAF [2, 3, 4].

The identification of the critical role of NLRP3 inflammasome in the maturation of these inflammatory cytokines prompted the study of its role in the pathogenesis of several syndromes. The term IL-1β dependent autoinflammatory syndromes has been adopted for such syndromes. This group of diseases is characterized by defective regulation of innate immune response and the absence of autoantibodies or antigen-specific T cells [5].

Dysregulation of NLRP3 inflammasome based on mutations of inflammasome related genes has been implicated in the pathogenesis of cryopyrin-associated periodic fever syndrome (CAPS), hyper-IgD syndrome (HIDS), pyogenic arthritis, pyoderma gangrrenosum, and acne syndrome (PAPA), or deficiency of IL-1 receptor antagonist (DIRA) [6]. Interestingly, NLRP3 inflammasome activation by danger signals such as monosodium urate (MSU), calcium pyrophosphate dehydrate (CPPD), amyloid-beta, glucose or silica and asbestos is proposed as a key molecular mechanism in diseases including gout, pseudogout, Altheimer's disease, pulmonary fibrosis or the 2 diabetes mellitus [5].

We discuss in this review about this new-coming entity of diseases along with the pitfall for understanding the pathphysiology.

NLRP3 inflammasome

Recognition of microorganisms by the innate immune system depends on conserved germ line-encoded receptors called pattern-recognition receptors (PRRs) that sense conserved motifs present on microbes named PAMPs [7].

PRRs are classified into three groups: secreted, trans-membrane and cytosolic (Fig. 1). Secreted PRRs such as collectins, ficolins and pentraxins bind microbes and activate the complement system. The trans-membrane PRRs are Toll-like receptors (TLRs) and the C-type lectins, with some members expressed on cell surface (such as TLR2/4 and Dectin1/2) and some expressed on endosome membrane (TLR3/7/9). The cytosolic PRRs include the RIG-I-like receptors (RLRs), the nucleotide-binding domain leucine-rich repeat containing receptors (NLRs) and the newly identified DNA sensors AIM2 (absent in melanoma 2) and IFI16 (interferon-inducible protein16) [8,9,10]. Although the RLRs mainly detect viral pathogens, the NLRs can detect both PAMPs and DAMPs [11]. In response to PAMPs or DAMPs, a subset of NLRs forms a complex with ASC (apoptosis-associated speck-like protein containing a CARD) to activate caspase-1 [12]. In 2002, Tschopp group first named this complex the inflammasome [13]. Up to date, at least 4 different inflammasomes have been identified; they are the NLRP1, NLRP3, IPAF (NLRC4) and AIM2 inflammasomes [14].

NLRP3, also called CIAS1, PYPAF1, Cryopyrin, CLR1.1 (CATERPILLAR 1.1) or NALP3, is one of the best characterized NLR family members. In mice, NLRP3 is mainly expressed in tissues such as lung, liver, kidney, colon and ovary, with particularly high expression in the skin and eye [15, 16]. Mouse neutrophils, peripheral blood mononuclear cells (PBMCs) and bone marrow-derived dendritic cells (BMDCs) express high level of NLRP3 constitutively, while the bone marrow- derived macrophages (BMDMs) and Th2 cells only express this molecule at moderate level [15, 16]. However, upon TLR or TNF receptor stimulation, the expression of NLRP3 in BMDMs is dramatically elevated, largely as a result of NF-κB

activation [16, 17]. Both mouse and human osteoblasts express NLRP3 [18]. In addition, primary human PBMCs, the monocyte-derived THP-1 cell line, primary human keratinocytes (PK), keratinocyte-derived HaCaT cells, primary mast cells (MS), granulocytes and B cells all express NLRP3 [19, 20, 21]. The tissue distribution of human NLRP3 is also found in the urothelial layer in the bladder and in epithelial cells lining the oral and genital tracts besides the skin cells mentioned above [20,21].

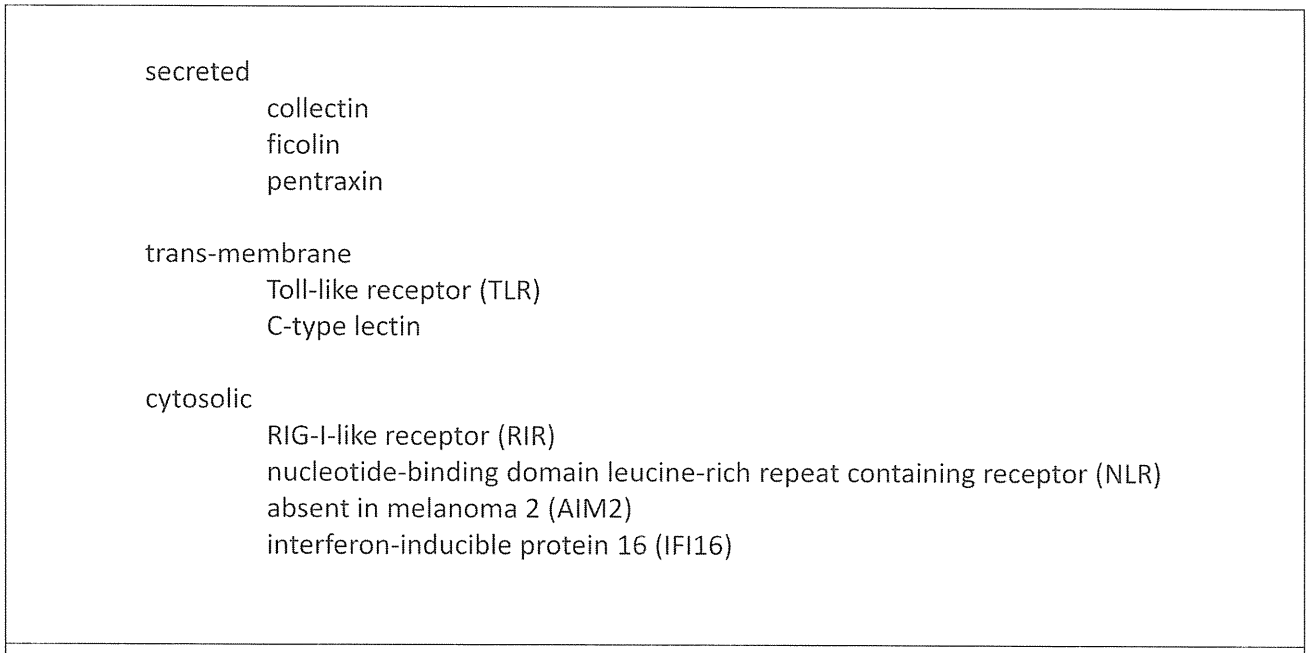

Fig. 1 Classification of pattern-recognition receptors

Recognition of microorganisms by the innate immune system depends on conserved germ line-encoded receptors called pattern-recognition receptors (PRRs) that sense conserved motifs present on microbes named PAMPs.
PRRs are classified into three groups: secreted, trans-membrane and cytosolic.

Structural analysis revealed that NLRP3 contains an N-terminal pyrin domain, an intermediate NACHT domain and a C-terminal LRR domain. Upon activation,NLRP3 recruits ASC via a pyrin-pyrindomain interaction and the recruited ASC binds to pro-caspase-1 via a CARD–CARD interaction. The multiprotein complex thus formed, now called the NLRP3 inflammasome, then activates caspase-1, and the latter cleaves pro-interleukin-1β (IL-1β) and pro-IL-18 to form mature IL-1β and IL-18, respectively (Fig. 2) [22]. Whole pathogens, PAMPs, DAMPs and environmental irritants can all activate the NLRP3 inflammasome. However, the exact mechanism(s) leading to NLRP3 inflammasome activation is still not clear. Given the diversity of these NLRP3 activators, a consensus is emerging that there is a common downstream intracellular activator that constitutes a final common pathway for NLRP3 activation (Fig. 2) [23,24]. In any case, the mature IL-1β and IL-18 production resulted from NLRP3 activation are highly potent proinflammatory mediators important for host defense against infectious agents. In addition, via IL-1β, the NLRP3 inflammasome is linked to Th17 cell differentiation [25,26] as well as to Th2 response since vaccination with aluminum adjutants also activates this inflammasome [27,28]. It should be noted, however, that NLRP3-mediated secretion of IL-1β and IL-18 must be under tight control, as excessive production of these cytokines can lead to autoinflammatory diseases. This is seen in the group of diseases collectively called cryopyrin(CIAS1, NLRP3)-associated periodic syndromes (CAPSs) which are caused by hyper-activation of the NLRP3 inflammasome due to mutations in the NLRP3 gene [29,30]. Besides, hyperimmunoglobulinemia D with periodic fever syndrome (HIDS), the deficiency of the IL-1 receptor antagonist (DIRA), and the syndrome of pyogenic arthritis with pyoderma gangrenosum and acne (PAPA) are caused by mutations in genes encoding proteins that directly or

indirectly correlate NLRP3 [8].

Cryopyrin-associated periodic syndrome (CAPS) or cryopyrinopathies

The cryopyrin-associated periodic syndrome spectrum, which encompass FCAS(Familial cold autoinflammatory syndrome), MWS(Muckle-Wells syndrome), and NOMID/CINCA syndrome (Neonatal onset multisystem inflammatory disease/chronic infantile neurologic, cutaneous, and articular syndrome), is caused by mutations in the cold induced autoinflammatory syndrome 1 (CIAS1) gene, first identified in 2001 [31]. CIAS1 codes for the protein cryopyrin, also known as NLRP3 or PYPAF1 [32]. We use the term NLRP3 thereafter. The cryopyrinopathies are transmitted in an autosomal dominant pattern. The NLRP3 gene is located on chromosome 1q44 and has 9 exons. Roughly 85% of NLRP3 mutations occur in exon 3 [29, 33]. Clinical manifestations vary among the three cryopyrinopathies, but several common features are often found, such as fever, pseudourticarial rash, joint involvement, and profoundly elevated inflammatory markers [32]. The most consistent finding across the CAPS spectrum is a migratory, maculopapular, urticaria-like, and usually nonpruritic rash. Skin biopsy reveals polymorphonuclear perivascular infiltration of the dermis, which contrasts with the biopsy findings of classical urticaria. The unique features of each of the cryopyrinopathies are described below [34].

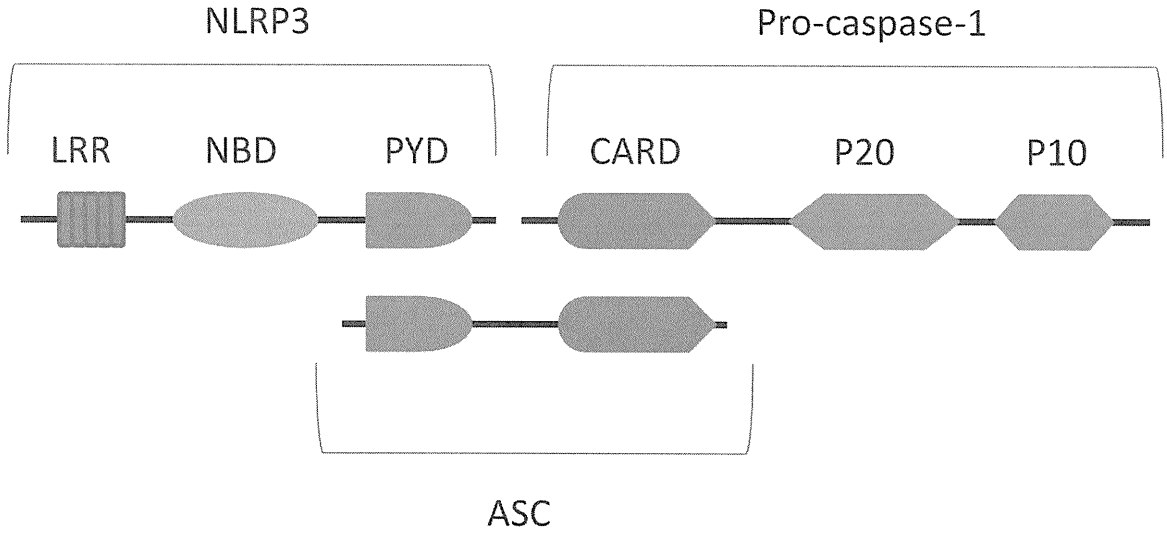

Figure 2 Schematic structure of NLRP3 inflammasome

Activation leads to the binding of NLRP3 with ACS through PYD-PYD interaction, resulting in recruiting of pro-caspase-1 via CARD-CARD interaction.

LRR: leucine-rich –repeat ; NBD:nucleotide-binding domain

PYD:pyrindomain; CARD:caspaseactivating and recruitment domain

a) Familial cold autoinflammatory syndrome (FCAS)

FCAS, also known as familial cold urticaria, is at the benign end of the CAPS spectrum, and has the most favorable prognosis of all the cryopyrinopathies [32, 35]. FCAS is characterized by episodes of low-grade fever, polyarthralgia, and nonpruritic pseudourticarial rash appearing 1-2 hours after cold exposure (range: 30 min to 6 h) and persisting for approximately 12 hours [37, 36]. Other commonly reported symptoms include conjunctivitis, profuse sweating, dizziness, headache, nausea, and extreme thirst. Symptoms are most intense in young adults, but may begin as early as childhood. Less commonly, the syndrome may present as recurrent fever, mild arthralgia, inflammatory cardiomyopathy, nephropathy, and thyroiditis, with no skin involvement. Secondary amyloidosis is

the main cause of death, occurring in up to 2% of cases [37]. Treatment includes prevention of cold exposure and, in more severe cases, anakinra. A recent study of rilonacept, a long-acting soluble receptor that binds IL-1, found good efficacy and safety in 44 patients with FCAS. NSAIDs and corticosteroids are variably effective, and antihistamines are not effective at all [38].

b) Muckle-Wells syndrome (MWS)

In 1962, Muckle & Wells described a familial syndrome of urticaria, deafness, and amyloidosis affecting nine individuals [39]. The symptoms of MWS arise in childhood, as an urticaria-like rash with low-grade fever and arthralgia. Recurring episodes of arthritis and conjunctivitis may also occur. The most characteristic manifestation of MWS is sensorineural hearing loss, which is due to chronic inflammation of the organ of Corti with cochlear nerve atrophy [40]. Less common findings include oral and genital ulcers, cystinuria, ichthyosis, recurrent abdominal pain, and microscopic hematuria. Secondary amyloidosis is common, and may occur in 1/3 to 1/4 of patients. A finding of NLRP3 mutation confirms the diagnosis. Other laboratory findings include thrombocytopenia, anemia, and increased levels of acute-phase reactants [41]. As in the other cryopyrinopathies, IL-1 receptor inhibition with anakinra can reverse the clinical manifestations of MWS, including hearing loss.

c) Neonatal onset multisystem inflammatory disease/chronic infantile neurologic, cutaneous, and articular syndrome (NOMID or CINCA syndrome)

NOMID, or CINCA syndrome, is the most severe phenotype of the cryopyrinopathy spectrum, and was first described by Prieur & Griscelli in 1981 [42]. The disease is characterized by a triad of rash, chronic aseptic meningitis, and arthropathy. Clinical manifestations arise in the first weeks of life; the cutaneous lesions often appear within hours of birth [43]. Inflammatory symptoms (such as fever) are practically continuous, with occasional flares, and affected children have severe growth retardation.

Skin lesions are found in nearly 100% of cases. CNS involvement is the second most common feature, typically presenting as chronic aseptic meningitis with leukocyte infiltration of the cerebrospinal fluid, which leads to a broad range of symptoms including chronic irritability, headaches, seizures, transient hemiplegia, and lower limb spasticity. If left untreated, approximately 80% of patients will develop sensorineural hearing loss and ocular disease, such as conjunctivitis, anterior and posterior uveitis, papilledema, and optic nerve atrophy with loss of vision [44]. Other findings include developmental delay and mental retardation. Patients with NOMID/CINCA syndrome have a typical facial appearance, characterized by frontal bossing, macrocrania, and saddle nose. The musculoskeletal changes of NOMID/CINCA syndrome can range from asymptomatic arthritis to deforming arthropathy. Most patients show inflammatory changes of the long-bone epiphyses and metaphyses, with abnormal epiphyseal calcification and cartilage overgrowth, leading to shortened limbs and joint deformities. Premature ossification of the patella, with symmetrical patellar overgrowth, is a characteristic finding [43]. The typical arthropathy of NOMID is found in 50% of patients [43].

Nonspecific laboratory changes are as in other autoinflammatory syndromes, and may include anemia, thrombocytosis, moderately increased white blood cell counts, and increased inflammatory markers, such as ESR and CRP levels. The diagnosis of NOMID/CINCA syndrome relies on adequate clinical suspicion and confirmatory genetic testing. However, only 50% of patients with a characteristic presentation of NOMID/CINCA syndrome have NLRP3 mutations, which suggests that other yet-unknown genes may also be involved in its pathophysiology.

Without early identification and treatment, the prognosis for patients with NOMID/CINCA syndrome is guarded. In addition to deforming articular involvement and neurologic sequelae, the disease carries a high risk of secondary amyloidosis in the few patients who live to adulthood. Anakinra, an IL-1 receptor antagonist, is currently the drug of choice for treatment of NOMID and has been widely used in this indication, providing significant improvement in all clinical manifestations of the disease and, consequently, patient quality of life [43]. Corticosteroids and NSAIDs can provide symptomatic relief, but have no effect on articular or neurologic involvement.

Recently, canakinumab, which targets selectively human IL-1ß with high affinity and prevents the cytokine from interaction to its receptor, is reported to effectively block the inflammatory response in CAPS. In all studies performed, canakinumab

showed a rapid improvement of symptoms of CAPS and a complete clinical response was achieved in most patients. Inflammatory markers such as C-reactive protein and serum amyloid-A protein were reduced to normal levels within few days. In comparison to other IL-1 blockers, canakinumab provides a longer plasma half-life and less injection site reactions [45, 46].

Mevalonate kinase deficiency (MKD) or hyper-IgD and periodic fever syndrome (HIDS)

HIDS follows an autosomal recessive pattern of inheritance, and is most often diagnosed in Northeastern Europe. The disease is caused by mutations in the MVK (mevalonate kinase) gene, which was discovered in 1999 [47]. MVK, which has 11 exons and is located on the long arm of chromosome 12 (locus 12q24), codes for mevalonate kinase (MK), a 396-amino acid-long enzyme. Most patients have a combination of two mutations, one of which is very often V377I. HIDS-associated mutations lead to a major reduction in MK activity (1 to 10% of normal levels), whereas mutations that completely eliminate MK function lead to a condition known as mevalonic aciduria (MA) [48, 49]. MA is a rare disease characterized by periodic fever with severe CNS involvement, mental retardation, ataxia, myopathy, poor growth, and early death.

MK plays an essential role in the isoprenoid and cholesterol synthesis pathways. It catalyzes the conversion of mevalonic acid to mevalonate 5-phosphate during the synthesis of molecules such as cholesterol, vitamin D, biliary salts, corticosteroids, and non-steroidal isoprenoid compounds. During cholesterol biosynthesis, 3-hydroxy-3-methylglutaryl-coenzyme A (HMG-CoA) reductase (the enzyme inhibited by statins) converts HMG-CoA to mevalonate, which is then phosphorylated to mevalonate phosphate. Mutations in the MVK gene block this pathway, preventing the conversion of mevalonate to mevalonate phosphate. The absence of a negative feedback loop, which is naturally provided by the presence of the end products of synthesis, leads to increased HMG-CoA reductase activity, consequently increasing serum, tissue, and urine levels of mevalonic acid. *In vitro* studies have shown that reduced synthesis of isoprenoids is associated with increased production of IL-1β [50]. Another recent in vitro study showed that MK inhibition leads to increased secretion of IL-1β due to activation of caspase-1, the enzyme that catalyzes formation of active IL-1β from its precursor [51]. High levels of immunoglobulin D (IgD) are characteristic of HIDS, but are apparently not associated with the severity of pathophysiology of the condition [52].

In MKD, febrile attacks occur more frequently in the first year of life, lasting 3 to 7 days and recurring every 4 to 6 weeks. However, the time elapsed between episodes can vary from patient to patient and even in a single individual. Febrile episodes recur for years, most frequently in childhood and adolescence, but months to years can go by between flares. Episodes may be triggered by immunization, trauma, surgery, or stress, and are characterized by high fever preceded by chills. Lymphadenopathy is extremely common. It is usually cervical, bilateral, and painful. Abdominal pain is also a frequent symptom, and may be accompanied by vomiting and/or diarrhea. Patients will also frequently report headache, and splenomegaly and hepatomegaly are common. Polyarthralgia and non-erosive arthritis of the large joints, particularly of the knees and ankles are also common. Arthritis is usually polyarticular and symmetric. Most patients have diffuse cutaneous lesions, which may consist of erythematous maculopapular rash, urticaria-like rash, erythematous nodules, petechiae, or purpura. Febrile episodes may be accompanied by sudden increase in acute phase reactant levels, including neutrophilic leukocytosis and elevated ESR, CRP, and SAA. Measurement of urinary mevalonate levels during attacks may be useful, particularly in patients with normal IgD levels.

IgD levels are persistently high (≥100 U/mL) in most patients. Nonetheless, IgD levels may be within normal limits in some HIDS patients, especially children under the age of 3 [52]. Furthermore, the finding of high IgD levels is not specific for HIDS, as it occurs in other inflammatory diseases, such as FMF and TRAPS.

The diagnosis of MKD is confirmed by a finding of MVK mutations. However, the presence of a clinical phenotype consistent with the disease in conjunction with high serum IgD and urinary mevalonate levels may suggest the diagnosis.

Most of the usual treatments, such as NSAIDs, corticosteroids, IVIG, colchicine, and thalidomide, are ineffective in HIDS. The involvement of MK in the cholesterol synthesis pathway has encouraged the introduction of statins in the management of MKD; the efficacy of simvastatin, an HMG-CoA reductase inhibitor, has been demonstrated in 5/6 of MKD pa-

tients [53]. Use of etanercept and anakinra in refractory cases has also been reported [54, 55, 56]. Recently two patients with MVA have been treated successfully with stem cell transplantation [57].

Pyogenic aseptic arthritis, pyoderma gangrenosum, and acne syndrome (PAPA syndrome)

PAPA syndrome is an autosomal dominant disease characterized by sterile, deforming arthritis, skin ulcers (pyoderma gangrenosum), and severe cystic acne. Unlike other autoinflammatory syndromes, PAPA does not have fever as its most prominent symptom.

PAPA syndrome is caused by mutations in the gene that codes proline-serine-threonine phosphatase interacting protein 1 (PSTPIP1), and only five associated mutations have been reported thus far. PSTPIP1 is a 416-amino acid-long protein expressed mostly in neutrophils. Mutations in PSTPIP1 are believed to lead to hyperphosphorylation of the protein, which could increase the potency of its binding to pyrin, with subsequent activation of IL-1β production, as seen in FMF [58].

Deficiency of interleukin-1–receptor antagonist (DIRA)

A new autosomal recessive AIS, caused by mutations in the IL1RN gene, which codes for interleukin-1 receptor antagonist (IL1Ra), was reported recently [59]. The syndrome, which was described in 10 patients, was given the name "deficiency of interleukin-1 receptor antagonist" (DIRA) and is characterized by early onset of symptoms, most frequently in the neonatal period.

Patients with DIRA present with pustulosis, multifocal aseptic osteomyelitis, and markedly elevated ESR and CRP levels. Skin involvement may range from sparse pustules to generalized pustular dermatitis or ichthyosiform lesions. Skin biopsy may reveal neutrophilic infiltration of the epidermis and dermis, pustules in the stratum corneum, acanthosis, and hyperkeratosis. All patients described in the report had osteomyelitis, characterized by pain with movement and periarticular swelling; the most frequent radiological findings were widening of the costal arches, periosteal elevation along long bones, and multifocal osteolytic lesions.

As in the other pyogenic autoinflammatory syndromes (PAPA and Majeed syndrome), fever is not a striking feature of DIRA, and was not present in any of the patients described. Two of the 10 patients had interstitial lung disease, and three died before therapy could be attempted (at 2 months, 21 months, and 9 years of age respectively).

The treatment of choice is recombinant IL-1RA (anakinra), which produces a dramatic response in skin and bone symptoms and in the quality of life of patients with DIRA.

Pitfall for diagnosis of NOMID/CINCA syndrome

Recent genetic studies revealed that CAPS patients usually carry heterozygous mutations in the NLRP3 coding region (mutation positive patients) [60, 61, 62, 63, 64, 65]. Although they exhibit no recognizable differences in clinical symptoms or in their response to treatment, approximately half of CINCA syndrome patients lack detectable mutations in NLRP3, as assessed by conventional genomic sequencing (mutation-negative patients) [32, 60, 61, 62, 66, 67], indicating the existence of genetic heterogeneity among CAPS patients. Recently, we reported a patient with CINCA syndrome exhibiting mosaicism of a disease-associated mutation of NLRP3 [68]. This case suggested that some mutation-negative CAPS patients might have mosaicism of the NLRP3 mutation; however, the contribution of NLRP3 mosaicism to disease is controversial. Aksentijevich et al claimed that NLRP3 mosaicism is a rare event in mutation-negative patients, based on their analysis of 14 patients in which NLRP3 mosaicism was not identified, even with careful bidirectional sequencing [32, 68].

Somatic mosaicism has been reported in a number of autosomal dominant monogenic diseases [69]. Diagnosis of mosaicism by conventional genomic sequencing using the dideoxy termination method is often difficult, because the overlapping chromatogram of the mutant is easily missed when the frequency of a mutant allele is less than 20% to 30%. Heteroduplex-based methods or subcloning-based analysis of mutant alleles enable one to detect such low-level mosaicism; however, these methods are resource intensive, and cannot distinguish whether the detected mutation is disease-causing or simply a nonfunctional single nucleotide polymorphism (SNP). An alternative approach involves the isolation of mutant cells using functional analyses based on their characteristic biologic features, and then determining the DNA sequence of the isolated cells. Based on these backgrounds, we set out to identify specific biologic features of NLRP3-mutant cells compared

with nonmutated cells, in an effort to specifically isolate NLRP3-mutated cells from mutation-negative patients [70].

Disease-associated NLRP3 mutations induce ASC-dependent NF-κB activation in some systems, and we reported that they also induce necrotic cell death in the human monocytic cell line THP-1, which is a novel function of NLRP3 [68]. Based on these backgrounds, we explored whether NLRP3-mutant cells have specific biologic features, using monocytes from mutation-positive patients, and found that NLRP3-mutant monocytes rapidly underwent necrosis-like cell death after treatment with lipopolysaccharide (LPS) to induce NLRP3 expression. This unique phenotype of NLRP3 mutant cells enabled us to differentiate NLRP3-mutated cells and nonmutated cells in 3 of 4 mutation-negative CAPS patients, and we were able to successfully demonstrate that these 3 patients had mutations of NLRP3 as latent mosaicism (Fig. 3) [71, 72].

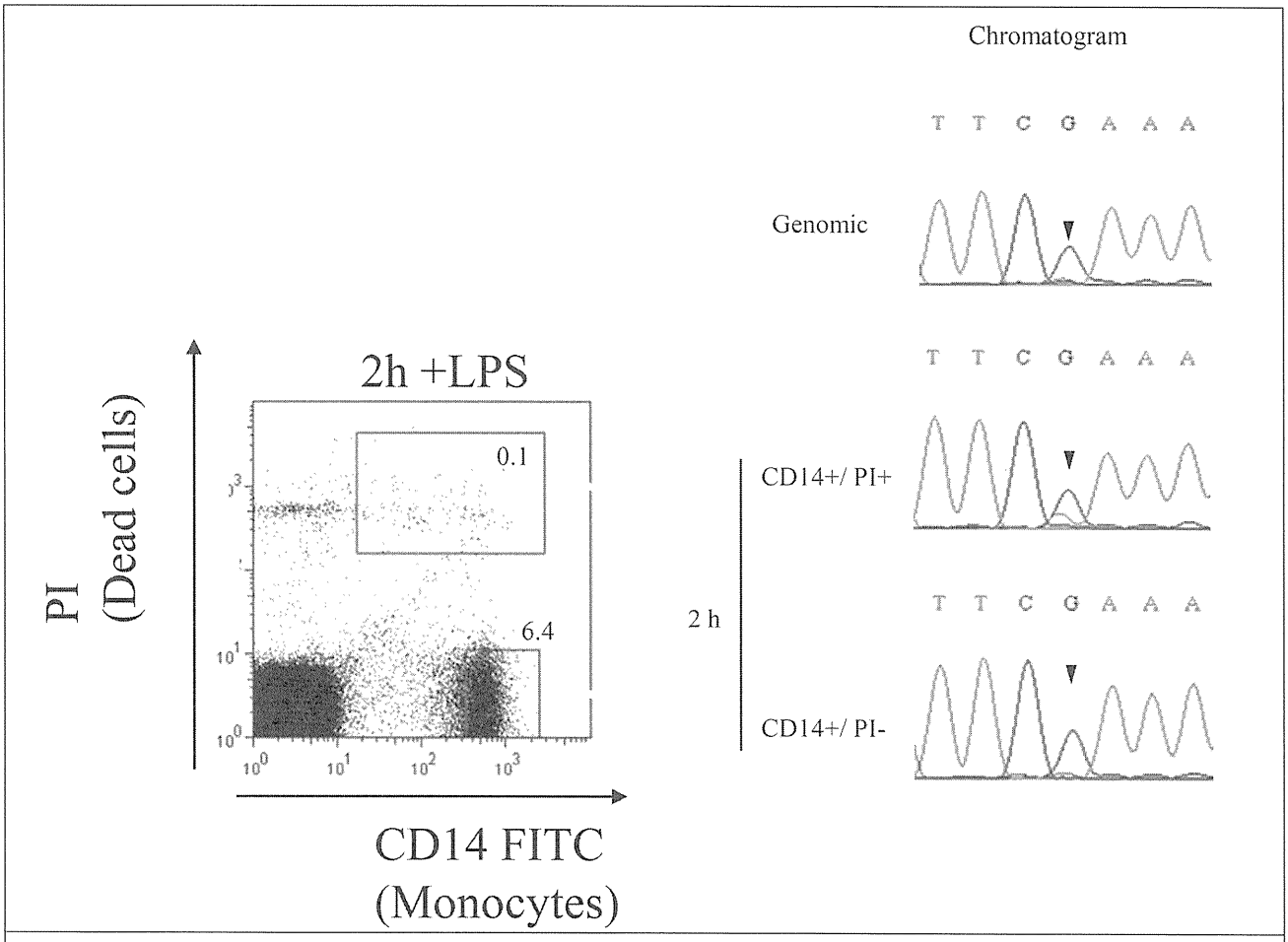

Fig. 3 Enrichment of dying monocytesin mutation-negative patient revealed latent overlapping peaks

PBMCs from mutation-negative CAPS patient were cultured with or without LPS (10 ng/mL) for 24 hours. CD14-positive and -negative cells were sorted, and DNA was extracted and sequenced for analysis of NLRP3.

Reference

1) Medzhitov R: new adventures of an old flame. Cell Inflammation. 2010; 140: 771-776.

2) FranchiL, Warner N, Viani K, Nunez G: Function of Nod-like receptors in microbial recognition and host defense. Immunol Rev. 2009; 227: 106-128.

3) Martinon F, Mayor A, Tschopp J: The inflammasomes: guardians of the body. Annu Rev. Immunol. 2009; 27: 229-265.

4) Mitroulis I, Skendros P, Ritis K: Targeting IL-1β in disease; the expanding role of NLRP3 inflammasome. Eur J Inter Med. 2010; 21: 157-163.

5) Masters LS, Simon A, Aksentijevich I, Kastner DL. Horror antoinflammaticus: the molecular pathphysiology of autoinflammatory disease. Annu Rev.

Immunol. 2009; 27: 621-628.

6) Kastner DL, Aksentijevich I, Goldbach-Mansky R. Autoinflammatory disease reloated: a clinical perspective. Cell. 2010; 140: 784-790.

7) Chen M, Wang H, Chen W, Meng G: Regulation of adaptive immunity by the NLRP3 inflammasome. Int Immunopharmacol. 2010; Nov 27. [Epub ahead of print]

8) Hornung V, Latz E: Intracellular recognition. Nat Rev. Immunol. 2010; 10: 123-130.

9) Unterholzner L, Keating SE, Baran M, Horan KA, Jensen SB, Sharma S, Sirois CM, Jin T, Latz E, Xiao TS, Fitzgerald KA, Paludan SR, Bowie AG: FI16 is an innate immune sensor for intracellular DNA. Nat Immunol. 2010; 11: 997-1004.

10) Iwasaki A, Medzhitov R: Regulation of adaptive immunity by the innate immune system. Science. 2010; 327: 291-295.

11) Takeuchi O, Akira S: Pattern recognition receptors and inflammation. Cell. 2010; 140: 805-820.

12) Franchi L, Eigenbrod T, Munoz-Planillo R, Nunez G: The inflammasome: a caspase- 1-activation platform that regulates immune responses and disease pathogenesis. Nat. Immunol. 2009; 10: 241-247.

13) Martinon F, Burns K, Tschopp J. The inflammasome: a molecular platform triggering activation of inflammatory caspases and processing of pro-IL-beta. Mol Cell. 2002; 10: 417-426.

14) Schroder K, Tschopp J: The inflammasomes. Cell. 2010; 140: 821-832.

15) Anderson JP, Mueller JL, Rosengren S, Boyle DL, Schaner P, Cannon SB, Goodyear CS, Hoffman HM: Structural, expression, and evolutionary analysis of mouse CIAS1. Gene. 2004; 338: 25-34.

16) Sutterwala FS, Ogura Y, Szczepanik M, Lara-Tejero M, Lichtenberger GS, Grant EP, Bertin J, Coyle AJ, Galán JE, Askenase PW, Flavell RA: Critical role for NALP3/CIAS1/Cryopyrin in innate and adaptive immunity through its regulation of caspase-1. Immunity. 2006; 24: 317-327.

17) Bauernfeind FG, Horvath G, Stutz A, Alnemri ES, MacDonald K, Speert D, Fernandes-Alnemri T, Wu J, Monks BG, Fitzgerald KA, Hornung V, Latz E. Cutting edge: NF-kappaB activating pattern recognition and cytokine receptors license NLRP3 inflammasome activation by regulating NLRP3 expression. J Immunol. 2009; 183: 787-791.

18) McCall SH, Sahraei M, Young AB, Worley CS, Duncan JA, Ting JP, Marriott I: Osteoblasts express NLRP3, a nucleotide-binding domain and leucine-rich repeat region containing receptor implicated in bacterially induced cell death. J Bone Miner Res. 2008; 23: 30-40.

19) Gattorno M, Tassi S, Carta S, Delfino L, Ferlito F, Pelagatti MA, D'Osualdo A, Buoncompagni A, Alpigiani MG, Alessio M, Martini A, Rubartelli A: Pattern of interleukin-1beta secretion in response to lipopolysaccharide and ATP before and after interleukin-1 blockade in patients with CIAS1 mutations. Arthritis Rheum. 2007; 56: 3138-3148.

20) Nakamura Y, Kambe N, Saito M, Nishikomori R, Kim YG, Murakami M, Núñez G, Matsue H: Mast cells mediate neutrophil recruitment and vascular leakage through the NLRP3 inflammasome in histamine-independent urticaria. J Exp Med. 2009; 206: 1037-1046.

21) Kummer JA, Broekhuizen R, Everett H, Agostini L, Kuijk L, Martinon F, van Bruggen R, Tschopp J: Inflammasome components NALP 1 and 3 show distinct but separate expression profiles in human tissues suggesting a site-specific role in the inflammatory response. J Histochem Cytochem. 2007; 55: 443-452.

22) Ogura Y, Sutterwala FS, Flavell RA. The inflammasome: first line of the immune response to cell stress. Cell. 2006; 126: 659-662.

23) Allen IC, Scull MA, Moore CB, Holl EK, McElvania-TeKippe E, Taxman DJ, Guthrie EH, Pickles RJ, Ting JP: The NLRP3 inflammasome mediates in vivo innate immunity to influenza A virus through recognition of viral RNA. Immunity. 2009; 30: 556-565.

24) Meng G, Strober W: New insights into the nature of autoinflammatory diseases from mice with Nlrp3 mutations. Eur J Immunol. 2010; 40: 649-653.

25) Chung Y, Chang SH, Martinez GJ, Yang XO, Nurieva R, Kang HS, Ma L, Watowich SS, Jetten AM, Tian Q, Dong C: Critical regulation of early Th17 cell differentiation by interleukin-1 signaling. Immunity. 2009; 30: 576-587.

26) Meng G, Zhang F, Fuss I, Kitani A, StroberW: A mutation in the Nlrp3 gene causing inflammasome

hyperactivation potentiates Th17 cell-dominant immune responses. Immunity. 2009; 30: 860-874.

27) Eisenbarth SC, Colegio OR, O'Connor W, Sutterwala FS, Flavell RA: Crucial role for the Nalp3 inflammasome in the immunostimulatory properties of aluminium adjuvants. Nature. 2008; 453: 1122-1126.

28) Spreafico R, Ricciardi-Castagnoli P, Mortellaro A: The controversial relationship between NLRP3, alum, danger signals and the next-generation adjuvants. Eur J Immunol. 2010; 40: 638-642.

29) Hoffman HM, Mueller JL, Broide DH, Wanderer AA, Kolodner RD: Mutation of a new gene encoding a putative pyrin-like protein causes familial cold autoinflammatory syndrome and Muckle–Wells syndrome. Nat Genet. 2001; 29: 301-305.

30) Ting JPY, Kastner DL, Hoffman HM: CATERPILLERs, pyrin and hereditary immunological disorders. Nat Rev Immunol. 2006; 6: 183-195.

31) Aksentijevich I, Nowak M, Mallah M, Chae JJ, Watford WT, Hofmann SR, Stein L, Russo R, Goldsmith D, Dent P, Rosenberg HF, Austin F, Remmers EF, Balow JE Jr, Rosenzweig S, Komarow H, Shoham NG, Wood G, Jones J, Mangra N, Carrero H, Adams BS, Moore TL, Schikler K, Hoffman H, Lovell DJ, Lipnick R, Barron K, O'Shea JJ, Kastner DL, Goldbach-Mansky R: De novo CIAS1 mutations, cytokine activation, and evidence for genetic heterogeneity in patients with neonatal-onset multisystem inflammatory disease (NOMID): a new member of the expanding family of pyrin-associated autoinflammatory diseases. Arthritis Rheum. 2002; 46: 3340-3348.

32) Aksentijevich I, D Putnam C, Remmers EF, Mueller JL, Le J, Kolodner RD, Moak Z, Chuang M, Austin F, Goldbach-Mansky R, Hoffman HM, Kastner DL: The clinical continuum of cryopyrinopathies: novel CIAS1 mutations in North American patients and a new cryopyrin model. Arthritis Rheum. 2007; 56: 1273-1285.

33) Aróstegui JI, Aldea A, Modesto C, Rua MJ, Argüelles F, González-Enseñat MA, Ramos E, Rius J, Plaza S, Vives J, Yagüe J: Clinical and genetic heterogeneity among Spanish patients with recurrent autoinflammatory syndromes associated with the CIAS1/PYPAF1/NALP3 gene. Arthritis Rheum. 2004; 50: 4045-4050

34) Jesus AA, Oliveira JB, Hilário MO, Terreri MT, Fujihira E, Watase M, Carneiro-Sampaio M, Silva CA: Pediatric hereditary autoinflammatory syndromes. J Pediatr (Rio J). 2010: 86; 353-366.

35) Jesus AA, Silva CA, Segundo GR, Aksentijevich I, Fujihira E, Watanabe M, Carneiro-Sampaio M, Duarte AJ, Oliveira JB. Phenotype-genotype analysis of cryopyrin-associated periodic syndromes (CAPS): description of a rare non-exon 3 and a novel CIAS1 missense mutation. J Clin Immunol. 2008; 28: 134-138.

36) Hoffman HM, Wanderer AA, Broide DH. Familial cold autoinflammatory syndrome: phenotype and genotype of an autosomal dominant periodic fever. J Allergy Clin Immunol. 2001; 108: 615-620.

37) Rigante D: Autoinflammatory syndromes behind the scenes of recurrent fevers in children. Med Sci Monit. 2009; 15: RA179-187.

38) Gandhi C, Healy C, Wanderer AA, Hoffman HM. Familial atypical cold urticaria: description of a new hereditary disease. J Allergy Clin Immunol. 2009; 124: 1245-1250.

39) Muckle TJ, Wells. Urticaria, deafness, and amyloidosis: a new heredo-familial syndrome. Q J Med. 1962; 31: 235-248.

40) Dodé C, Le Dû N, Cuisset L, Letourneur F, Berthelot JM, Vaudour G, Meyrier A, Watts RA, Scott DG, Nicholls A, Granel B, Frances C, Garcier F, Edery P, Boulinguez S, Domergues JP, Delpech M, Grateau G: New mutations of CIAS1 that are responsible for Muckle-Wells syndrome and familial cold urticaria: a novel mutation underlies both syndromes. Am J Hum Genet. 2002; 70: 1498-1506.

41) Hawkins PN, Lachmann HJ, Aganna E, McDermott MF: Spectrum of clinical features in Muckle-Wells syndrome and response to anakinra. Arthritis Rheum. 2004; 50: 607-612.

42) Prieur AM, Griscelli C: Arthropathy with rash, chronic meningitis, eye lesions, and mental retardation. J Pediatr. 1981; 99: 79-83.

43) Goldbach-Mansky R, Dailey NJ, Canna SW, Gelabert A, Jones J, Rubin BI, Kim HJ, Brewer C, Zalewski C, Wiggs E, Hill S, Turner ML, Karp BI, Aksentijevich I, Pucino F, Penzak SR, Haverkamp MH, Stein L, Adams BS, Moore TL, Fuhlbrigge RC, Shaham B, Jarvis JN, O'Neil K, Vehe RK, Beitz LO, Gardner G, Hannan WP, Warren RW, Horn W, Cole

JL, Paul SM, Hawkins PN, Pham TH, Snyder C, Wesley RA, Hoffmann SC, Holland SM, Butman JA, Kastner DL: Neonatal-onset multisystem inflammatory disease responsive to interleukin-1beta inhibition. N Engl J Med. 2006; 355: 581-592.

44) Neven B, Prieur AM, Quartier dit Maire P; Medscape: Cryopyrinopathies: update on pathogenesis and treatment. Nat Clin Pract Rheumatol. 2008; 4: 481-489.

45) Feist E, Burmester GR: Canakinumab for treatment of cryopyrin-associated periodic syndrome. Expert Opin Biol Ther. 2010; 10: 1631-1636.

46) Toker O, Hashkes PJ: Critical appraisal of canakinumab in the treatment of adults and children with cryopyrin-associated periodic syndrome (CAPS). Biologics. 2010; 25: 131-138.

47) Houten SM, Kuis W, Duran M, de Koning TJ, van Royen-Kerkhof A, Romeijn GJ, et al: Mutations in MVK, encoding mevalonate kinase, cause hyperimmunoglobulinaemia D and periodic fever syndrome. Nat Genet. 1999; 22: 175-177.

48) Prieur AM: A recently recognised chronic inflammatory disease of early onset characterised by the triad of rash, central nervous system involvement and arthropathy. Clin Exp Rheumatol. 2001; 19: 103-106.

49) McTaggart SJ: Isoprenylated proteins. Cell Mol Life Sci. 2006; 63: 255-267.

50) Frenkel J, Rijkers GT, Mandey SH, Buurman SW, Houten SM, Wanders RJ, Waterham HR, Kuis W: Lack of isoprenoid products raises ex vivo interleukin-1beta secretion in hyperimmunoglobulinemia D and periodic fever syndrome. Arthritis Rheum. 2002; 46: 2794-2803.

51) Normand S, Massonnet B, Delwail A, Favot L, Cuisset L, Grateau G, Morel F, Silvain C, Lecron JC: Specific increase in caspase-1 activity and secretion of IL-1 family cytokines: a putative link between mevalonate kinase deficiency and inflammation. Eur Cytokine Netw. 2009; 20: 101-107.

52) Ammouri W, Cuisset L, Rouaghe S, Rolland MO, Delpech M, Grateau G, Ravet N: Diagnostic value of serum immunoglobulinaemia D level in patients with a clinical suspicion of hyper IgD syndrome. Rheumatology (Oxford). 2007; 46: 1597-1600.

53) Simon A, Drewe E, van der Meer JW, Powell RJ, Kelley RI, Stalenhoef AF, Drenth JP: Simvastatin treatment for inflammatory attacks of the hyperimmunoglobulinemia D and periodic fever syndrome. Clin Pharmacol Ther. 2004; 75: 476-483.

54) Bodar EJ, van der Hilst JC, Drenth JP, van der Meer JW, Simon A: Effect of etanercept and anakinra on inflammatory attacks in the hyper-IgD syndrome: introducing a vaccination provocation model. Neth J Med. 2005; 63: 260-264.

55) Nevyjel M, Pontillo A, Calligaris L, Tommasini A, D'Osualdo A, Waterham HR, Granzotto M, Crovella S, Barbi E, Ventura A: Diagnostics and therapeutic insights in a severe case of mevalonate kinase deficiency. Pediatrics. 2007; 119: e523-527.

56) Topaloglu R, Ayaz NA, Waterham HR, Yuce A, Gumruk F, Sanal O: Hyperimmunoglobulinemia D and periodic fever syndrome: treatment with etanercept and follow-up. Clin Rheumatol. 2008; 27: 1317-1320.

57) Neven B, Valayannopoulos V, Quartier P, Blanche S, Prieur AM, Debré M, Rolland MO, Rabier D, Cuisset L, Cavazzana-Calvo M, de Lonlay P, Fischer A: Allogeneic bone marrow transplantation in mevalonic aciduria. N Engl J Med. 2007; 356: 2700-2703.

58) Shoham NG, Centola M, Mansfield E, Hull KM, Wood G, Wise CA, Kastner DL: Pyrin binds the PSTPIP1/CD2BP1 protein, defining familial Mediterranean fever and PAPA syndrome as disorders in the same pathway. Proc Natl Acad Sci U S A. 2003; 100: 13501-13506.

59) Aksentijevich I, Masters SL, Ferguson PJ, Dancey P, Frenkel J, van Royen-Kerkhoff A, Laxer R, Tedgård U, Cowen EW, Pham TH, Booty M, Estes JD, Sandler NG, Plass N, Stone DL, Turner ML, Hill S, Butman JA, Schneider R, Babyn P, El-Shanti HI, Pope E, Barron K, Bing X, Laurence A, Lee CC, Chapelle D, Clarke GI, Ohson K, Nicholson M, Gadina M, Yang B, Korman BD, Gregersen PK, van Hagen PM, Hak AE, Huizing M, Rahman P, Douek DC, Remmers EF, Kastner DL, Goldbach-Mansky R: An autoinflammatory disease with deficiency of the interleukin-1-receptor antagonist. N Engl J Med. 2009; 360: 2426-2437.

60) Aksentijevich I, Nowak M, Mallah M, Chae JJ, Watford WT, Hofmann SR, Stein L, Russo R, Goldsmith D, Dent P, Rosenberg HF, Austin F, Remmers EF, Balow JE Jr, Rosenzweig S, Komarow H, Sho-

ham NG, Wood G, Jones J, Mangra N, Carrero H, Adams BS, Moore TL, Schikler K, Hoffman H, Lovell DJ, Lipnick R, Barron K, O'Shea JJ, Kastner DL, Goldbach-Mansky R: De novo CIAS1 mutations, cytokine activation, and evidence for genetic heterogeneity in patients with neonatal-onset multisystem inflammatory disease (NOMID): a new member of the expanding family of pyrin-associated autoinflammatory diseases. Arthritis Rheum. 2002; 46: 3340-3348.

61) Feldmann J, Prieur AM, Quartier P, Berquin P, Certain S, Cortis E, Teillac-Hamel D, Fischer A, de Saint Basile G: Chronic infantile neurological cutaneous and articular syndrome is caused by mutations in CIAS1, a gene highly expressed in polymorphonuclear cells and chondrocytes. Am J Hum Genet. 2002; 71: 198-203.

62) Neven B, Callebaut I, Prieur AM, Feldmann J, Bodemer C, Lepore L, Derfalvi B, Benjaponpitak S, Vesely R, Sauvain MJ, Oertle S, Allen R, Morgan G, Borkhardt A, Hill C, Gardner-Medwin J, Fischer A, de Saint Basile G: Molecular basis of the spectral expression of CIAS1 mutations associated with phagocytic cell-mediated autoinflammatory disorders CINCA/NOMID, MWS, and FCU. Blood. 2004; 103: 2809-2815.

63) Hoffman HM, Mueller JL, Broide DH, Wanderer AA, Kolodner RD: Mutation of a new gene encoding a putative pyrin-like protein causes familialcold autoinflammatory syndrome and Muckle-Wells syndrome. Nat Genet. 2001; 29: 301-305.

64) Aganna E, Martinon F, Hawkins PN, Ross JB, Swan DC, Booth DR, Lachmann HJ, Bybee A, Gaudet R, Woo P, Feighery C, Cotter FE, Thome M, Hitman GA, Tschopp J, McDermott MF: Association of mutations in the NALP3/CIAS1/PYPAF1 gene with a broad phenotype including recurrent fever, cold sensitivity, sensorineural deafness, and AA amyloidosis. Arthritis Rheum. 2002; 46: 2445-2452.

65) Dodé C, Le Dû N, Cuisset L, Letourneur F, Berthelot JM, Vaudour G, Meyrier A, Watts RA, Scott DG, Nicholls A, Granel B, Frances C, Garcier F, Edery P, Boulinguez S, Domergues JP, Delpech M, Grateau G: New mutations of CIAS1 that are responsible for Muckle-Wells syndrome and familial cold urticaria: a novel mutation underlies both syndromes. Am J Hum Genet. 2002; 70: 1498-1506.

66) Aróstegui JI, Aldea A, Modesto C, Rua MJ, Argüelles F, González-Enseñat MA, Ramos E, Rius J, Plaza S, Vives J, Yagüe J: Clinical and genetic heterogeneity among Spanish patients with recurrent autoinflammatory syndromes associated with the CIAS1/PYPAF1/NALP3 gene. Arthritis Rheum. 2004; 50: 4045-4050.

67) Goldbach-Mansky R, Dailey NJ, Canna SW, Gelabert A, Jones J, Rubin BI, Kim HJ, Brewer C, Zalewski C, Wiggs E, Hill S, Turner ML, Karp BI, Aksentijevich I, Pucino F, Penzak SR, Haverkamp MH, Stein L, Adams BS, Moore TL, Fuhlbrigge RC, Shaham B, Jarvis JN, O'Neil K, Vehe RK, Beitz LO, Gardner G, Hannan WP, Warren RW, Horn W, Cole JL, Paul SM, Hawkins PN, Pham TH, Snyder C, Wesley RA, Hoffmann SC, Holland SM, Butman JA, Kastner DL: Neonatal-onset multisystem inflammatory disease responsive to interleukin-1beta inhibition. N Engl J Med. 2006; 355: 581-592.

68) Aksentijevich I, Remmers EF, Goldbach-Mansky R, Reiff A, Kastner DL: Mutational analysis in neonatal-onset multisystem inflammatory disease: Comment on the articles by Frenkel et al and Saito et al. Arthritis Rheum. 2006; 54: 2703- 2704.

69) Youssoufian H, Pyeritz RE: Mechanisms and consequences of somatic mosaicism in humans. Nat Rev Genet. 2002; 3: 748-758.

70) Fujisawa A, Kambe N, Saito M, Nishikomori R, Tanizaki H, Kanazawa N, Adachi S, Heike T, Sagara J, Suda T, Nakahata T, Miyachi Y: Disease-associated mutations in CIAS1 induce cathepsin B-dependent rapid cell death of human THP-1 monocytic cells. Blood. 2007; 109: 2903-2911.

71) Saito M, Fujisawa A, Nishikomori R, Kambe N, Nakata-Hizume M, Yoshimoto M, Ohmori K, Okafuji I, Yoshioka T, Kusunoki T, Miyachi Y, Heike T, Nakahata T: Somatic mosaicism of CIAS1 in a patient with chronic infantile neurologic, cutaneous, articular syndrome. Arthritis Rheum. 2005; 52: 3579-3585.

72) Saito M, Nishikomori R, Kambe N, Fujisawa A, Tanizaki H, Takeichi K, Imagawa T, Iehara T, Takada H, Matsubayashi T, Tanaka H, Kawashima H, Kawakami K, Kagami S, Okafuji I, Yoshioka T, Adachi S, Heike T, Miyachi Y, Nakahata T: Disease-associated CIAS1 mutations induce monocyte death, revealing low-level mosaicism in mutation-negative cryopyrin-associated periodic syndrome patients. Blood. 2008; 111: 2132-2141.

A Novel Serum-Free Monolayer Culture for Orderly Hematopoietic Differentiation of Human Pluripotent Cells via Mesodermal Progenitors

Akira Niwa[1,2], Toshio Heike[2], Katsutsugu Umeda[2,4], Koichi Oshima[1], Itaru Kato[1,2], Hiromi Sakai[5], Hirofumi Suemori[3], Tatsutoshi Nakahata[1,2], Megumu K. Saito[1,2]*

1 Clinical Application Department, Center.for iPS Cell Research and Application, Kyoto University, Kyoto, Japan, **2** Department of Pediatrics, Graduate School of Medicine, Kyoto University, Kyoto, Japan, **3** Laboratory of Embryonic Stem Cell Research, Stem Cell Research Center, Institute for Frontier Medical Sciences, Kyoto University, Kyoto, Japan, **4** Institute of Molecular Medicine, University of Texas Health Science Center, Houston, Texas, United States of America, **5** Waseda Bioscience Research Institute in Helios, Singapore

Abstract

Elucidating the *in vitro* differentiation of human embryonic stem (ES) and induced pluripotent stem (iPS) cells is important for understanding both normal and pathological hematopoietic development *in vivo*. For this purpose, a robust and simple hematopoietic differentiation system that can faithfully trace *in vivo* hematopoiesis is necessary. In this study, we established a novel serum-free monolayer culture that can trace the *in vivo* hematopoietic pathway from ES/iPS cells to functional definitive blood cells via mesodermal progenitors. Stepwise tuning of exogenous cytokine cocktails induced the hematopoietic mesodermal progenitors via primitive streak cells. These progenitors were then differentiated into various cell lineages depending on the hematopoietic cytokines present. Moreover, single cell deposition assay revealed that common bipotential hemoangiogenic progenitors were induced in our culture. Our system provides a new, robust, and simple method for investigating the mechanisms of mesodermal and hematopoietic differentiation.

Citation: Niwa A, Heike T, Umeda K, Oshima K, Kato I, et al. (2011) A Novel Serum-Free Monolayer Culture for Orderly Hematopoietic Differentiation of Human Pluripotent Cells via Mesodermal Progenitors. PLoS ONE 6(7): e22261. doi:10.1371/journal.pone.0022261

Editor: Dan Kaufman, University of Minnesota, United States of America

Received January 4, 2011; **Accepted** June 18, 2011; **Published** July 27, 2011

Funding: This work was supported by grants from the Ministry of Education, Culture, Sports, Science, and Technology of Japan (#22790979). The funders had no role in study design, data collection and analysis, decision to publish, or preparation of the manuscript.

Competing Interests: The authors have declared that no competing interests exist.

* E-mail: msaito@kuhp.kyoto-u.ac.jp

Introduction

Because of pluripotency and self-renewal, human embryonic stem (ES) cells and induced pluripotent stem (iPS) cells are potential cell sources for regenerative medicine and other clinical applications, such as cell therapies, drug screening, toxicology, and investigation of disease mechanisms [1,2,3]. iPS cells are reprogrammed somatic cells with ES cell-like characteristics that are generated by introducing certain combinations of genes, proteins, or small molecules into the original cells [4,5,6,7]. Patient-derived iPS cells have facilitated individualized regenerative medicine without immunological or ethical concerns. Moreover, patient- or disease-specific iPS cells are an important resource for unraveling human hematological disorders. However, for this purpose, a robust and simple hematopoietic differentiation system that can reliably mimic in vivo hematopoiesis is necessary.

Mesodermal and hematopoietic differentiation is a dynamic event associated with changes in both the location and phenotype of cells [8,9,10,11]. Some primitive streak (PS) cells appearing just after gastrulation form the mesoderm, and a subset of mesodermal cells differentiate into hematopoietic cell lineages [9,12,13,14,15,16]. Previous studies have accumulated evidence on these embryonic developmental pathways.

The leading methods of blood cell induction from ES/iPS cells employ 2 different systems: monolayer animal-derived stromal cell coculture and 3-dimensional embryoid body (EB) formation. Both methods can produce hematopoietic cells from mesodermal progenitors, and combinations of cytokines can control, to some extent, the specific lineage commitment [1,2,17,18,19,20,21,22,23,24,25,26,27,28]. In the former method, a previous study showed that OP9 stromal cells, which are derived from the bone marrow of osteopetrotic mice, augment the survival of human ES cell-derived hematopoietic progenitors [29]. However, as the stromal cell condition controls the robustness of the system, it can be relatively unstable. Furthermore, the induction of hematopoietic cells from human pluripotent cells on murine-derived cells is less efficient than that from mice cells.

In EB-based methods, hematopoietic cells emerge from specific areas positive for endothelial markers such as CD31 [30,31,32]. Through these methods, previous studies have generated a list of landmark genes for each developmental stage, such as *T* and *KDR* genes for the PS and mesodermal cells, respectively [12,16,17,18,25,28,33,34,35,36], and also have emphasized appropriate developmental conditions consisting of specific microenvironments, signal gradients, and cytokines given in suitable combinations with appropriate timing. For robust and reproducible specification to myelomonocytic lineages of cells, some recent studies have converted to serum-independent culture by using EB formation [37]. However, the difficulty in applying 3-dimensional location information inside EBs prevents substantial increases in

hematopoietic specification efficacy. Additionally, the sphere-like structure of the EB complicates tracking and determination of hematopoietic–stromal cell interactions.

To overcome these issues, we established a novel serum-free monolayer hematopoietic cell differentiation system from human ES and iPS cells. Although there are no reports describing the shift of human ES/iPS cells from primitive to definitive erythropoiesis in a monolayer xeno-cell-free condition, our system can trace the in vitro differentiation of human ES/iPS cells into multiple lineages of definitive blood cells, such as functional erythrocytes and neutrophils. Hematopoietic cells arise via an orderly developmental pathway that includes PS cells, mesoderm, and primitive hematopoiesis.

Materials and Methods

Maintenance of human ES/iPS cells in serum-free condition

Experiments were carried out with the human ES cell lines KhES-1 and KhES-3 (kindly provided by Norio Nakatsuji) and iPS cell lines 201B7 and 253G4 (kindly provided by Shinya Yamanaka). Stable derivatives of ES cells carrying the transgene for green fluorescent protein (GFP) after CAG promoter were also used [38,39]. The ES/iPS cells were maintained on a tissue culture dish (#353004; Becton-Dickinson, Franklin Lakes, NJ) coated with growth factor-reduced Matrigel (#354230; Becton-Dickinson) in mTeSR1 serum-free medium (#05850; STEMCELL Technologies, Vancouver, BC, Canada). The medium was replaced everyday. Passage was performed according to the manufacturer's protocol.

Differentiation of ES/iPS cells

First, undifferentiated ES/iPS cell colonies were prepared at the density of less than 5 colonies per well of a 6-well tissue culture plate (#353046; Becton-Dickinson). When individual colony grew up to approximately 500 μm in diameter, mTeSR1 maintenance medium was replaced by Stemline II serum-free medium (#S0192; Sigma-Aldrich, St. Louis, MO) supplemented with Insulin-Transferrin-Selenium-X Supplement (ITS) (#51500-056; Invitrogen, Carlsbad, CA). This day was defined as day 0 of differentiation. BMP4 (#314-BP-010; R&D Systems, Minneapolis, MN) was added for first 4 days and replaced by $VEGF_{165}$ (#293-VE-050; R&D Systems) and SCF (#255-SC-050; R&D Systems) on day 4. On day 6, the cytokines were again replaced by the haematopoietic cocktail described in the result section. Concentration of each cytokine was as follows: 20 ng/mL BMP4, 40 ng/mL $VEGF_{165}$, 50 ng/mL SCF, 10 ng/mL TPO (#288-TPN-025; R&D Systems), 50 ng/mL IL3 (#203-IL-050; R&D Systems), 50 ng/mL Flt-3 ligand (#308-FK-025; R&D Systems), 50 ng/mL G-CSF (#214-CS-025; R&D Systems), 50 ng/mL complex of IL-6 and soluble IL-6 receptor (FP6) (kindly provided by Kyowa Hakko Kirin Co., Ltd., Tokyo, Japan) and 5 IU/mL EPO (#329871; EMD Biosciences, San Diego, CA). Thereafter, the medium was changed every 5 days.

Antibodies

The primary murine anti-human monoclonal antibodies used for flow cytometric (FCM) analysis are as follows: PE-conjugated anti-SSEA-4 (#330405; BioLegend, San Diego, CA), Alexa Fluor® 647-conjugated anti-TRA-1-60 (#560122; Becton-Dickinson), biotin-conjugated anti-CD140a (#323503; Biolegend), Alexa Fluor® 647-conjugated anti-KDR (#338909; BioLegend), PE-conjugated anti-CXCR4 (#555974; Becton-Dickinson), PE-conjugated anti-CD117 (#313203; BioLegend), PE-conjugated CD34 (#A07776; Beckman Coulter, Brea, CA), FITC-conjugated CD43 (#560978; Becton-Dickinson), and APC-conjugated CD45 (#IM2473; Beckman Coulter). A streptavidin-PE (#554061; Becton Dickinson) was used as secondary antibody against biotin-conjugated primary antibody. The primary antibodies used to immunostain the colonies and floating blood cells included anti-human Oct3/4 (#611203; Becton-Dickinson), T (#sc-101164; Santa Cruz Biotechnology, Santa Cruz, CA), KDR (#MAB3571; R&D Systems), VE-Cadherin (#AF938; R&D Systems), and rabbit anti-pan-human Hb (#0855129; MP Biomedicals, Solon, OH). FITC-conjugated donkey anti-rat antibodies and Cy3-conjugated goat anti-mouse antibodies (Jackson ImmunoResearch Laboratories, Inc., West Grove, PA) were used as secondary antibodies.

Cytostaining

Floating cells were centrifuged onto glass slides by using a Shandon Cytospin 4 Cytocentrifuge (Thermo, Pittsburgh, PA) and analysed by microscopy after staining with May–Giemsa or myeloperoxidase. For immunofluorescence staining, cells fixed with 4% paraformaldehyde were first permeabilized with phosphate-buffered saline containing 5% skimmed milk (Becton–Dickinson) and 0.1% Triton X-100 and then incubated with primary antibodies, followed by incubation with FITC or Cy3-conjugated secondary antibodies. Nuclei were counterstained with 4,6-diamidino-2-phenylindole (DAPI) (Sigma-Aldrich).

Flow cytometric analysis

The adherent cells were treated with Dispase (#354235; Becton-Dickinson) and harvested by gently scraping the culture dish. Aggregated cell structure was chopped by a pair of scissors, processed by GentleMACS (Milteny Biotec, Germany) and then dispersed by 40-μm strainers (#2340; Becton-Dickinson) before staining with antibodies. Dead cells were excluded by DAPI staining. Samples were analysed using a MACSQuant (Milteny Biotec) and FlowJo software (Thermo). Cell sorting was performed using a FACSVantage or FACSAria (Becton–Dickinson).

RNA extraction and real-time quantitative PCR analysis

RNA samples were prepared using silica gel membrane-based spin-columns (RNeasy Mini-KitTM; Qiagen, Valencia, CA) and subjected to reverse transcription (RT) with a Sensiscript-RT Kit (Qiagen). All procedures were performed according to the manufacturer's instructions. For real-time quantitative PCR, primers and the fluorogenic probes were designed and selected according to Roche Universal Primer library software (Roche Diagnostics) and MGB probe system (Applied Biosystems, Carlsbad, CA). The instrument used was the Applied Biosystems ABIPrism 7900HT sequence detection system, and the software for data collection and analysis was SDS2.3. A GAPDH RNA probe (Hs00266705_g1) was used to normalise the data.

Clonogenic colony-forming assay

At the indicated days of culture, from days 6 through 25, the adherent cells were treated with dispase and harvested. They were incubated in a new tissue-culture dish (#3003, Becton–Dickinson) for 10 min to eliminate adherent non-haematopoietic cells [40]. Floating cells were collected and dispersed by 40-μm strainers. After dead cells were eliminated by labeling with Dead-Cert Nanoparticles (#DC-001, ImmunoSolv, Edinburgh, UK), live hematopoietic cells were cultured at a concentration of 1×10^3 (for counting CFU-G) or 10^4 (for counting CFU-Mix, BFU-E, and CFU-GM) cells/ml in 35-mm petri dishes (#1008; Becton-Dickinson) using

1 ml/dish of MethoCult GF+ semisolid medium (#4435; STEMCELL Technologies) as previously described. Colonies were counted after 14–21 days of incubation, and colony types were determined according to the criteria described previously [41,42,43] by in situ observation using an inverted microscope. The abbreviations used for the clonogenic progenitor cells are as follows: CFU-Mix, mixed colony-forming units; BFU-E, erythroid burst-forming units; CFU-GM, granulocyte–macrophage colony-forming units; and CFU-G, granulocyte colony-forming units.

Single-cell deposition assay

The single-cell deposition assay was performed as described previously [17,18,28]. In brief, single sorted cells were deposited in individual wells of 96-well plates with confluent OP9 layers and cultured for 14 days. Wells were scored by morphological observation for hematopoietic colony detection and stained with anti-vascular endothelial cadherin (VE-cadherin) antibodies for endothelial lineage detection.

Chemotaxis assay

Chemotaxis assay was performed with modified Boyden chamber method using 3.0-μm pore size cell culture inserts (Becton Dickinson). In brief, 5×10^4 cells harvested from floating cell fraction at day 25 were added to the upper chamber and induced to migrate towards the lower chamber containing 10 nM formyl-Met-Leu-Phe (fMLP; Sigma-Aldrich) for 4 hours at 37°C. After incubation, the cells in the lower chamber were collected and counted using a MACSQuant flow cytometer (Miltenyi Biotec). For quantitative analysis, equivalent amount of 6-μm beads (Becton Dickinson) were added to each FCM sample, and the cell numbers were determined by measuring the ratio of cells to beads.

Phagocytosis and detection of reactive oxygen species

Phagocytosis and production of reactive oxygen species were detected by chemiluminescent microspheres (luminol-binding carboxyl hydrophilic microspheres; TORAY, Tokyo, Japan) as described previously [44]. In brief, 2×10^4 floating cells were suspended in 50 μL of the reaction buffer (HBSS containing 20 mM *N*-2-hydroxyethylpiperazine-*N*-2-ethanesulfonic acid (HEPES)) per tube. To activate the system, 5 μl chemiluminescent microspheres were added, and light emission was recorded continuously using a luminometer (TD-20/20; Turner Designs, Sunnyvale, CA). During the measurement, samples were kept at 37°C. To inhibit the reaction, 1.75 μg of cytochalasin B (Sigma-Aldrich) was added to the samples.

Measurement of oxygen-binding ability

Floating blood cells derived from KhES-1 and 253G4 strains were harvested on day 32 of differentiation (with erythropoietic cytokine cocktail). Oxygen dissociation curves for hemoglobin were measured using a Hemox-Analyzer (TCS Scientific Corporation, New Hope, PA) as previously reported [45,46].

Results

Stepwise generation of functional hematopoietic cells from human ES/iPS cells in the serum-free monolayer culture without animal-derived stromal cells

To assess the differentiation activity of each human ES/iPS cell line with high reproducibility, we used a chemically defined medium in the monolayer differentiation culture and succeeded in inducing various blood cells, including erythrocytes and neutrophils (Figure 1a). To present the developmental process from human ES/iPS cells to blood cells in an orderly manner, we divided the entire process into 3 steps: (1) initial differentiation into PS cells, (2) induction of the hematopoietic mesoderm (Movie S1), and (3) commitment to the hematopoietic lineages (Movie S2).

Step 1: Induction of PS-like cells from undifferentiated human ES/iPS cells with BMP4 (days 0–4). First, we examined the efficacy of initial progression from undifferentiated pluripotent cells (KhES-1) into PS-like cells according to the expression of representative marker genes, such as *T* and *Mixl1* (Figure 1b), and the change in morphology (Figure 1c). Without cytokines, these genes were only slightly upregulated during the first 4 days. However, when 40 ng/mL BMP4 was added to the culture, the expression levels of these genes increased, which is compatible with previous reports on the importance of BMP4 in mesodermal/endodermal differentiation via PS during early embryogenesis (Figure 1b). Further, transcription levels of the undifferentiated marker *Nanog* decreased. During this period, the colonies showed substantial morphological changes at the margins, and cell density decreased and cell contact diminished (Movie S1, Figure 1c). Immunohistochemical staining assays confirmed the upregulation of T and the lateral mesodermal marker, KDR, and downregulation of Oct3/4 (Figure 1c). However, regarding ectodermal commitment, the representative marker gene *Sox1* was hardly detected on day 4 in the presence of BMP4 (Figure 1b).

To assess the role of BMP4 in this step, we analyzed the differentiation efficacy of individual ES (KhES-1 and KhES-3) and iPS (201B7 and 253G4) cell strains with various concentrations of BMP4 in the presence or absence of its inhibitor, Noggin. As shown in Figure 1d, *T* gene expression was upregulated by BMP4 dose-dependently up to 20 ng/mL and was almost completely suppressed by the BMP4 inhibitor, Noggin, in both ES and iPS cells. This suggested that BMP4 was critical at this stage. From these results, we used BMP4 at 20 ng/mL concentration in subsequent experiments.

We also assayed the expression of several cell surface protein markers in this step (Figure 1e). On day 4, undifferentiated cell markers (TRA-1-60 and SSEA4) were downregulated, whereas paraxial and lateral mesoderm cell markers (CD140a and KDR) and markers for mesodermal and hematopoietic progenitors (CXCR4 and CD117) were upregulated. The early-phase hematopoietic-committed cell markers (CD34 and CD43) were still negative at this stage. Similar results were obtained for both ES and iPS cells (data not shown), suggesting that our system initiated paraxial and lateral mesodermal differentiation from pluripotent stem cells during Step 1 [33].

Step 2: Generation of $KDR^+CD34^+CD45^-$ progenitors with VEGF and SCF (days 4–6). Our previous studies of primate ES cells demonstrated that $KDR^+CD34^+CD45^-$ mesodermal progenitors derived in a VEGF-containing culture on OP9 stromal cells included hematopoietic progenitors [17,18]. Therefore, we used this data to induce these progenitors in our culture system. Considering the partial expression of KDR and CD117 during the first step, we replaced BMP4 with 40 ng/mL $VEGF_{165}$ (ligand for KDR) and 50 ng/mL SCF (ligand for CD117) on day 4 to accelerate selective differentiation to the lateral mesoderm with hematopoietic activities (Figure 1a).

During the next 2 days, the colonies exhibited 2 distinct regions: a plateau-like central area with stratified components and a surrounding area with monolayer cells (Movie S1, Figure 1c). On day 6, the mRNA expression pattern indicated the dominance of mesodermal cells rather than endodermal or ectodermal lineages

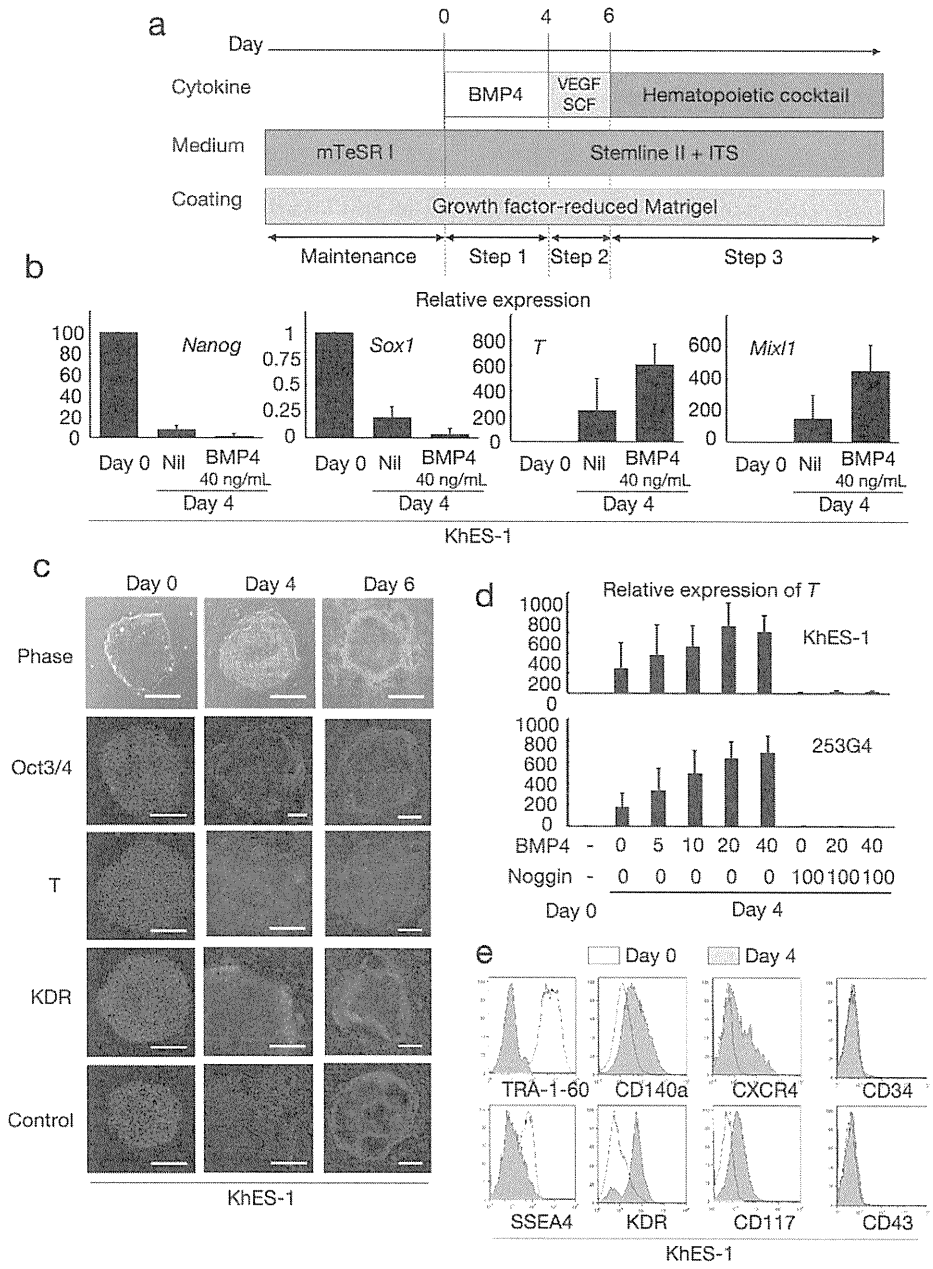

Figure 1. Blood cell induction from pluripotent stem cells starts with commitment into primitive streak. a. A schema of stepwise haematopoietic differentiation of human ES/iPS cells. **b.** Gene expression analysis of colonies at the beginning of differentiation (day 0) and the end of step 1 (day 4) with/without 40 ng/mL BMP4. Data from KhES-1 are shown as representative. **c.** Phase contrast microscopies and immunofluorescence staining of colonies during initial differentiation. Data from KhES-1 are shown as representative. **d.** Relative expression of *T* at day 4 of differentiation with different combinations of BMP4 and its inhibitor Noggin. Where shown, bars represent standard deviation of the mean of three independent experiments; Scale bars, 500 μm. Data from KhES-1 and 253G4 strains are shown as representative. **e.** Flow cytometric analysis of differentiating cells on day 4, indicating the down-regulation of immature cell markers and up-regulation of differentiated progenitor markers. Data from KhES-1 are shown as representative.
doi:10.1371/journal.pone.0022261.g001

(Figure 2a), and flow cytometric (FCM) analysis demonstrated the emergence of new cell fractions that were positive for KDR, CD117, CXCR4, and CD34 but negative for CD140a, CD43, and CD45 (Figure 2b). Our system robustly supports mesodermal induction from both ES and iPS cells, despite differences in efficacy among cell strains (Figure 2c).

Further, immunohistochemical staining for KDR indicated an uneven distribution of KDR^+ cells at the marginal zone of the plateau area (Figure 1c), suggesting that differentiation polarity within the colonies resulted in site-specific emergence of putative hematopoietic mesodermal progenitors.

Step 3: Production of functional blood cells dependent on cytokine cocktails (day 6 onward). On day 6, we changed the culture medium to another chemically defined medium containing hematopoietic cytokines (Figure 1a). To achieve lineage-directed differentiation, we used 2 combinations of cytokines: a myeloid-

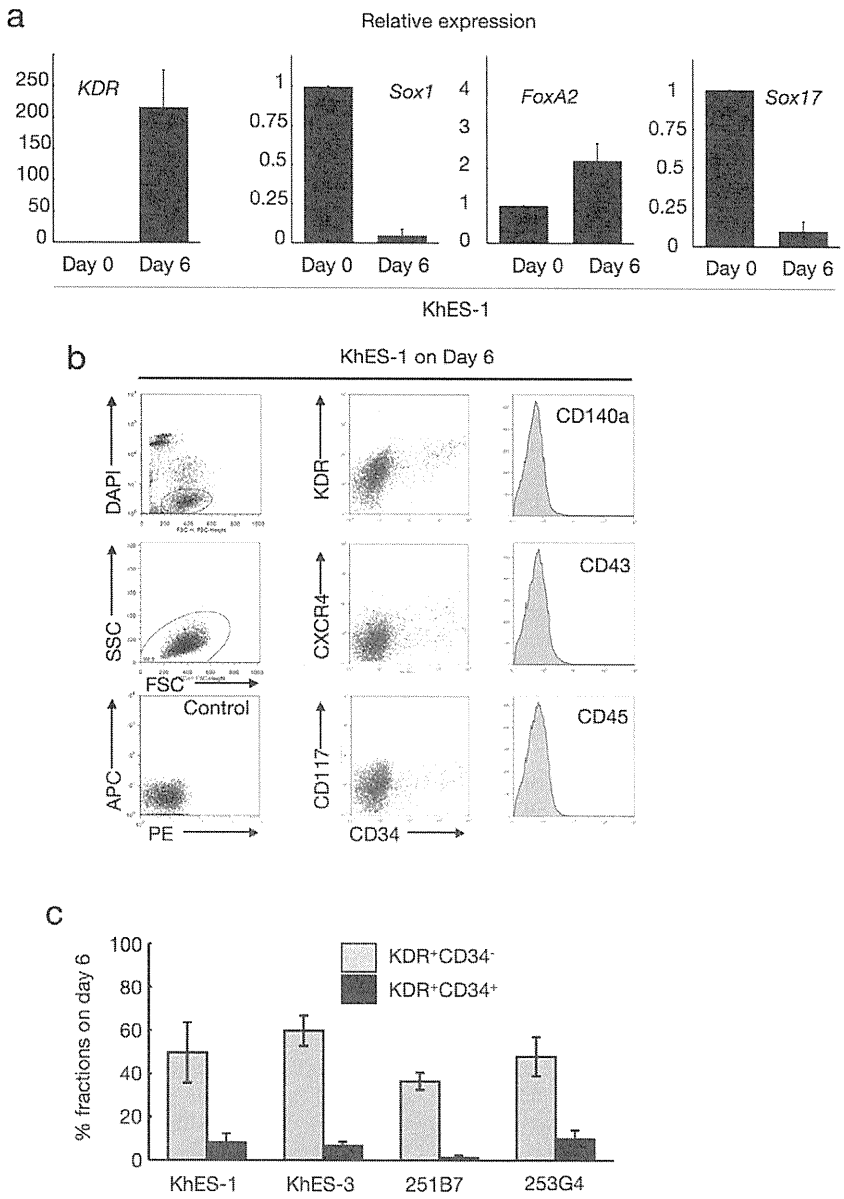

Figure 2. Characterization of cells during initial differentiation with lineage-specific marker expression. a. Expression analysis of lineage-specific marker genes at the beginning of differentiation (day 0) and the end of step 2 (day 6). Bars represent standard deviation of the mean of three independent experiments. Data from KhES-1 are shown as representative. **b.** The development of progenitors on day 6 positive for lateral mesoderm markers but negative for paraxial mesoderm and haematopoietic cell markers. Leftmost column shows the gating strategy for eliminating dead cells and debris. Data from KhES-1 are shown as representative. c. Efficacy of inducing $KDR^{+}CD34^{+\ or\ -}$ mesodermal progenitors from each two lines of human ES cells and iPS cells. Bars represent standard deviation of the mean of three independent experiments.
doi:10.1371/journal.pone.0022261.g002

induction cocktail containing SCF, TPO, IL3, FLT-3 ligand, and G-CSF; and an erythropoietic-differentiation cocktail containing SCF, TPO, IL3, FP6, and EPO.

Regardless of the cocktails, the colonies first exhibited a rosary-like appearance, with small sac-like structures aligned along the margins of the plateau areas, and grew for several days (Figure 3a, left panel). Hematopoietic cell clusters emerged from the edge of these structures on days 10–12, followed by the appearance of floating blood cells a few days later, which increased thereafter; hematopoietic clusters grew in size and number, and some exhibited areas with a cobblestone-like appearance (Figure 3a, right 3 panels; Movie S2). When fresh medium with the cytokines was supplied every 5 days, blood cell production was observed in both ES and iPS cell experiments until day 50 of differentiation, whereas few hematopoietic cells appeared without the cytokines (data not shown).

As expected, the myeloid-induction cocktail induced myelomonocytic lineages predominantly positive for CD45. Blood cells harvested on day 30 exhibited morphology compatible with myelomonocytic precursors and mature neutrophils, and displayed positive myeloperoxidase staining (Figure 3b). On the other hand, the erythropoietic-differentiation cocktail yielded cell lineages that included hemoglobin-positive (Hb^{+}) erythroid cells and $CD41^{+}$ megakaryocytes (Figure 3b). In the KhES-1 strain (3.5 [standard deviation (SD) = 1.5] undifferentiated colonies 250 μmm in diameter were initially plated in individual wells of 6-well plates